Catalysis Today 146 (2009) 71–75

Contents lists available at ScienceDirect

Catalysis Today

journal homepage: www.elsevier.com/locate/cattod

Combined reforming of methane over co-precipitated Ni–CeO_2, Ni–ZrO_2 and Ni–$Ce_{0.8}Zr_{0.2}O_2$ catalysts to produce synthesis gas for gas to liquid (GTL) process

Hyun-Seog Roh [a,*], Kee Young Koo [b], Wang Lai Yoon [b,*]

[a] Department of Environmental Engineering, Yonsei University, 234 Maeji, Heungeop, Wonju, Gangwon-do 220-710, South Korea
[b] Strategic Technologies Research Division, Korea Institute of Energy Research (KIER), 71-2 Jang-dong, Yuseong, Daejeon 305-343, South Korea

ARTICLE INFO

Article history:
Available online 31 January 2009

Keywords:
Co-precipitation
Ce–ZrO_2
Combined reforming
Synthesis gas
GTL

ABSTRACT

Ni–CeO_2, Ni–ZrO_2 and Ni–$Ce_{0.8}Zr_{0.2}O_2$ catalysts have been prepared by a co-precipitation method to develop catalysts suitable for synthesis gas production for gas to liquid (GTL) process. A conventional impregnation method was also employed to prepare Ni/CeO_2, Ni/ZrO_2 and Ni/$Ce_{0.8}Zr_{0.2}O_2$ catalysts to compare the impregnated catalysts with the co-precipitated ones. Ni content was fixed at 15% for both cases. It has been confirmed that the co-precipitated Ni–CeO_2 and Ni–$Ce_{0.8}Zr_{0.2}O_2$ catalysts exhibited relatively high activity as well as stability, while the impregnated Ni/CeO_2 and Ni/$Ce_{0.8}Zr_{0.2}O_2$ catalysts slowly deactivated with time on stream at 800 °C. At the temperature range from 700 to 750 °C, co-precipitated Ni–$Ce_{0.8}Zr_{0.2}O_2$ catalyst showed higher CH_4 and CO_2 conversion than Ni–CeO_2 catalyst. The enhanced catalytic activity and stability of the co-precipitated Ni–$Ce_{0.8}Zr_{0.2}O_2$ catalyst is due to the combination of nano-crystalline nature of cubic $Ce_{0.8}Zr_{0.2}O_2$ support and finely dispersed nano-sized NiO crystallites resulting in intimate contact between Ni and support, better Ni dispersion, and enhanced oxygen transfer during the reaction.

© 2009 Elsevier B.V. All rights reserved.

1. Introduction

Recently, a lot of research interest has been focused on gas to liquids (GTLs) technology due to high oil price (>$140/bbl). In general, GTL technology has three unit processes. Three unit processes are synthesis gas production, Fischer–Tropsch (F–T) synthesis and product work-up. Economically, the synthesis gas production unit is the most expensive of the three process sections. Thus, the design of the synthesis gas production unit is very important for the economics of a GTL project [1].

Commercially, synthesis gas has been produced from steam reforming of hydrocarbons [2–6]. However, steam reforming by itself is not suitable technology to produce synthesis gas for the GTL applications because the H_2/CO ratio from steam reforming of hydrocarbons deviates from 2, which is suitable for the F–T synthesis. Catalytic oxy-reforming of methane has also been considered to produce the synthesis gas with a H_2/CO ratio of 2 due to mild exothermicity, very short residence time, and fast start-up [7–11]. However, it has not been commercialized because of explosion danger and difficulty in controlling the operation [3].

Combined steam and carbon dioxide reforming of methane (CSCRM) can be considered as an alternative to produce synthesis gas with flexible H_2/CO ratio [12–16]. It is reported that it is easy to adjust H_2/CO ratio in the product synthesis gas to meet the requirements of downstream chemicals by controlling feed H_2O/CO_2/CH_4 ratio [13]. As a consequence, expensive air separation unit (ASU) in the synthesis gas production unit can be omitted by employing CSCRM, which makes the GTL process economically feasible process.

The breakthrough of CSCRM is to develop Ni catalysts with high coke resistance. It is known that supported Ni catalysts easily deactivate due to carbon formation in CSCRM [13]. Thus, it is an emerging topic to develop catalysts with high activity and stability for the target reaction. It has been reported that the Ni catalyst supported by small nanoparticles of ZrO_2, MgO, and Ce–ZrO_2 could be highly active and stable for dry reforming of methane ($CO_2 + CH_4 = 2H_2 + 2CO$: CRM) [12,17–19]. Roh et al. [13] also reported that nano-sized Ni/MgO–Al_2O_3 catalyst exhibited high activity with stability in CSCRM. As a consequence, it has been found that support plays a very important role in catalytic activity and stability in CSCRM.

It is known that Ce_{1-x}–Zr_xO_2 solid solution has high oxygen storage capacity, redox property, and thermal stability due to the partial substitution of Ce^{4+} with Zr^{4+} in the lattice of CeO_2 [20–22]. As a result, the Ce_{1-x}–Zr_xO_2 system has been considered as a

* Corresponding authors.
E-mail addresses: hsroh@yonsei.ac.kr (H.-S. Roh), wlyoon@kier.re.kr (W.L. Yoon).

0920-5861/$ – see front matter © 2009 Elsevier B.V. All rights reserved.
doi:10.1016/j.cattod.2009.01.001

promising support in methane reforming reactions [23–25]. Lercher et al. [26] reported that Pt/ZrO_2 exhibited excellent performance in CRM. Li et al. [27,28] reported that Ni/ZrO_2 catalysts showed high activity in CRM under diluted reaction conditions. Roh et al. [29,30] applied $Ni/Ce_{0.2}–Zr_{0.8}O_2$ for methane reforming reactions. Montoya et al. [31] applied Ni supported on a tetragonal $CeO_2–ZrO_2$ support for the CRM reaction. Roh et al. [32–35] also reported that $Rh/Ce–ZrO_2$ was highly active and selective in low temperature ethanol steam reforming. Song and co-workers applied CeO_2-supported Ni–Rh bimetallic catalysts for low temperature reforming of ethanol [36,37]. Jun and co-workers reported that a co-precipitation method was highly effective method to prepare $Ni–Ce–ZrO_2$ catalyst for CRM [38,39]. Very recently, co-precipitated $Ni–Ce–ZrO_2$ catalysts with various CeO_2/ZrO_2 ratios have been prepared and applied for CSCRM. The optimum CeO_2/ZrO_2 ratio has been found to be 4/1 (mol/mol) in CSCRM for the GTL process [16].

In this study, co-precipitated $Ni–CeO_2$, $Ni–ZrO_2$ and $Ni–Ce_{0.8}Zr_{0.2}O_2$ catalysts have been prepared and compared with the impregnated catalysts having the same composition in CSCRM to develop the active and stable catalysts for the target reaction.

2. Experimental

$Ni–CeO_2$, $Ni–ZrO_2$ and $Ni–Ce_{0.8}Zr_{0.2}O_2$ catalysts were prepared by a co-precipitation method (Ni loading = 15 wt.%). Stoichiometric quantities of zirconyl nitrate solution (20 wt.% in ZrO_2 base, MEL Chemicals), Ce-nitrate (99.9%, Aldrich) and Ni-nitrate (97%, Junsei Chemicals) were dissolved in distilled water, and the resulting solution was transferred to a round bottom flask. 10% KOH aqueous solution was employed as a precipitation agent. An aqueous solution of 10% KOH was added drop-wise at 80 °C until the pH of the solution reached 10.5. The solution was aged at 80 °C for 3 days. The detailed preparation procedure was described elsewhere [19]. The prepared catalysts were calcined in air at 800 °C for 6 h. For comparison, Ni/CeO_2, Ni/ZrO_2 and $Ni/Ce_{0.8}Zr_{0.2}O_2$ catalysts were prepared by the conventional impregnation method. This was done by impregnating appropriate amounts of $Ni(NO_3)_2{\cdot}6H_2O$ onto supports prepared by the co-precipitation method. The prepared catalysts were also calcined in air at 800 °C for 6 h.

The BET specific surface area was measured by nitrogen adsorption at −196 °C using a Micromeritics (ASAP-2000) surface area measurement apparatus. The XRD patterns were recorded using a Rigaku D/MAX-IIIC diffractometer (Ni filtered Cu Kα radiation, 40 kV, 50 mA). Pulse chemisorptions were performed in a multifunction apparatus. About 50 mg of catalyst was placed in a quartz reactor. Before pulse chemisorption, the sample was reduced in 5% H_2/Ar at 700 °C for 3 h. Then the sample was purged in Ar at 720 °C for 1 h and cooled to 50 °C in flowing Ar. Hydrogen was pulsed over the catalyst to measure the chemisorption at 50 °C using 5% H_2/Ar and continued at 8 min intervals until the area of the hydrogen peak on the chromatograph was identical.

Activity tests were carried out using a fixed-bed micro-reactor. Each catalyst was reduced in the reactor with 5% H_2/N_2 at 700 °C for 3 h prior to each catalytic activity measurement. The feed $H_2O/CO_2/CH_4$ ratio was fixed at 0.8/0.4/1.0 because product H_2/CO ratio of 2 was obtained in this reaction condition. A space velocity of 265,000 cm^3 gas fed/g_{cat}-h was employed to screen the catalysts. Effluent gases from the reactor were analyzed by an on-line gas chromatograph (HP 6890N) equipped with a thermal conductivity detector (TCD). The detailed experimental procedure was described elsewhere [13].

3. Results and discussion

3.1. Characterization

Table 1 summarizes the characteristics of catalysts prepared by co-precipitation and impregnation method. All the catalysts were calcined at 800 °C for 6 h. The co-precipitated $Ni–Ce_{0.8}Zr_{0.2}O_2$ catalyst shows the highest BET surface area. It indicates that the cubic $Ni–Ce_{0.8}Zr_{0.2}O_2$ catalyst has higher BET surface area than $Ni–CeO_2$ or $Ni–ZrO_2$. Compared with the impregnated catalysts, the co-precipitated catalysts show higher BET surface areas. This suggests that Ni incorporation during the synthesis procedure results in the development of fine nano-crystallites. As a result, support crystallite size of the co-precipitated catalysts is smaller than that of the impregnated ones. Especially, NiO crystallite size of the co-precipitated catalysts is much smaller than that of the impregnated ones. In the case of co-precipitated $Ni–Ce_{0.8}Zr_{0.2}O_2$ and $Ni–CeO_2$ catalysts, NiO crystallite size cannot be measured due to very broad and weak XRD peaks. This indicates that Ni is incorporated into the support lattice during the co-precipitation procedure, which is in good agreement with the previous result by Montoya et al. [31]. As a consequence, the reduction degrees of the co-precipitated catalysts are much lower than those of the impregnated ones. The Ni dispersion follows in the order: $Ni–Ce_{0.8}Zr_{0.2}O_2 > Ni–CeO_2 > Ni–ZrO_2 > Ni/Ce_{0.8}Zr_{0.2}O_2 > Ni/ZrO_2 > Ni–CeO_2$. Thus, it has been confirmed that the co-precipitation method is very effective to achieve high surface area as well as high Ni dispersion. By the way, the characteristics of the co-precipitated catalysts are different from the previous results [18]. In general, the surface areas of the co-precipitated catalysts in this study are higher than those of the literature [18]. This is mainly due to the fact that 10% KOH solution has been employed as a precipitation agent instead of 20% KOH solution and 10% KOH was added drop-wise very slowly to avoid rapid change of the pH of the solution. As a consequence, the dispersion values of the co-precipitated catalysts are relatively higher than those of the literature [18].

Fig. 1 shows XRD patterns of fresh co-precipitated and impregnated catalysts. Both co-precipitated $Ni–Ce_{0.8}Zr_{0.2}O_2$ and

Table 1
Characteristics of catalysts prepared by co-precipitation and impregnation method.

Catalyst	Surf. area (m^2/g)[a]	Support size (nm)[b]	NiO size (nm)[b]	Reduction degree (%)	Ni dispersion (%)[c]
$Ni–Ce_{0.8}Zr_{0.2}O_2$	97	9	N.A.[d]	53.7	6.60
$Ni–CeO_2$	67	14	N.A.[d]	61.8	6.40
$Ni–ZrO_2$	61	4	4	63.3	2.11
$Ni/Ce_{0.8}Zr_{0.2}O_2$	60	11	24	74.4	1.73
Ni/CeO_2	9	36	55	94.4	0.39
Ni/ZrO_2	17	24	21	99.0	0.50

[a] Estimated from N_2 adsorption at −196 °C (error <0.5).
[b] Estimated from XRD (error <0.5).
[c] Estimated from H_2 chemisorption at 50 °C considering reduction degree (error <0.005).
[d] Not available due to very broad and weak XRD peaks.

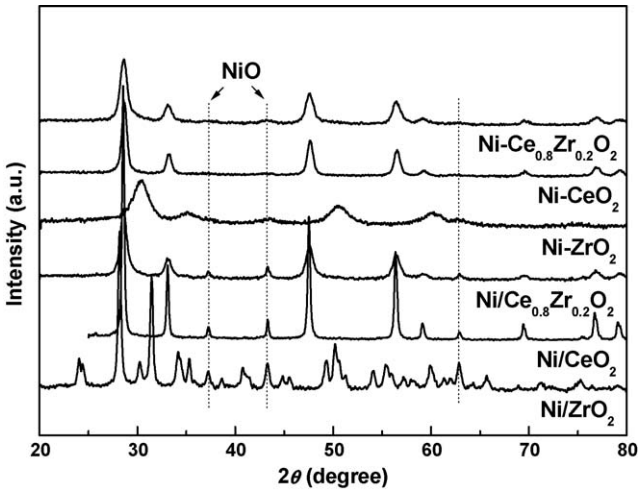

Fig. 1. XRD patterns of fresh co-precipitated and impregnated catalysts.

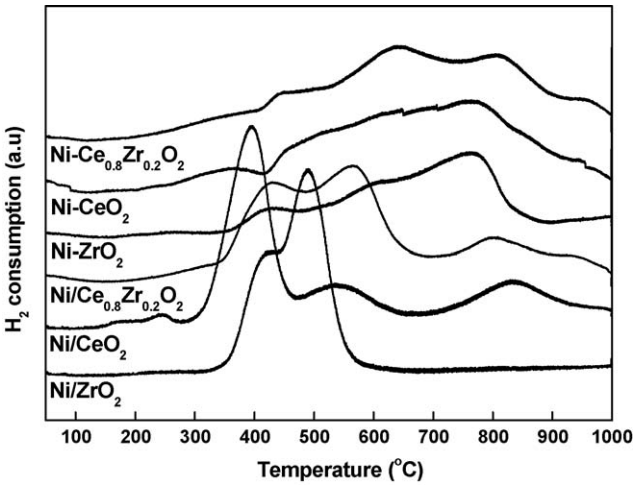

Fig. 3. TPR patterns of co-precipitated and impregnated catalysts.

Ni–CeO_2 catalysts give all characteristic reflections corresponding to cubic phase [19]. In both cases, the NiO peaks are too broad to calculate NiO crystallite size, indicating fine nano-dispersion of NiO on support. On the other hand, the Ni–ZrO_2 catalyst shows all characteristic reflections corresponding to tetragonal phase [4]. The crystallite size of NiO is the same as that of support (4 nm). The patterns of the impregnated Ni/$Ce_{0.8}Zr_{0.2}O_2$ catalyst are close to those of the co-precipitated Ni–$Ce_{0.8}Zr_{0.2}O_2$ catalyst. However, the NiO crystallite size of the impregnated Ni/$Ce_{0.8}Zr_{0.2}O_2$ catalyst is found to be 24 nm, which is much bigger than that of the co-precipitated one. For the Ni/CeO_2 catalyst, the patterns are corresponding to cubic structure of CeO_2 and NiO. On the other hand, the Ni/ZrO_2 catalyst shows characteristic peaks corresponding to monoclinic phase [4].

Fig. 2 shows XRD patterns of reduced catalysts. Both co-precipitated Ni–$Ce_{0.8}Zr_{0.2}O_2$ and Ni–CeO_2 catalysts do not show Ni peaks. This indicates that Ni is finely dispersed after the reduction process. This is in good agreement with the Ni dispersion data in Table 1. On the contrary, the Ni–ZrO_2 catalyst shows relatively sharp Ni peaks. Compared with the co-precipitated catalysts, Ni peaks of the impregnated catalysts are sharper than those of co-precipitated catalysts. This is also in good agreement with the dispersion data in Table 1.

Fig. 3 describes TPR patterns of co-precipitated and impregnated catalysts. It is known that the lower temperature peaks are assigned to the reduction of relatively free NiO species, while the higher temperature peaks are attributed to the reduction of complex NiO species, which have strong metal to support interaction (SMSI) [4,5]. Ni/CeO_2 shows sharp reduction peak at about 400 °C followed by a small tail. The first peak can be assigned to free NiO species. There is another peak at 830 °C due to partial reduction of CeO_2, which is consistent with the TPR curve of only CeO_2 support [10]. For Ni/ZrO_2, reduction peaks with maxima at about 420 and 490 °C are observed. The former can be assigned to relatively free NiO species and the latter to complex NiO species. In the case of Ni/$Ce_{0.8}Zr_{0.2}O_2$ catalyst, there are three peaks. The first peak is attributed to free NiO species. The second peak with maxima at 570 °C is assigned to complex NiO species. Ni to support interaction of this catalyst is stronger than that of Ni/ZrO_2 because the reduction peak is 80 °C higher than that of Ni/ZrO_2. The last peak is assigned to the reduction of segregated CeO_2 [19].

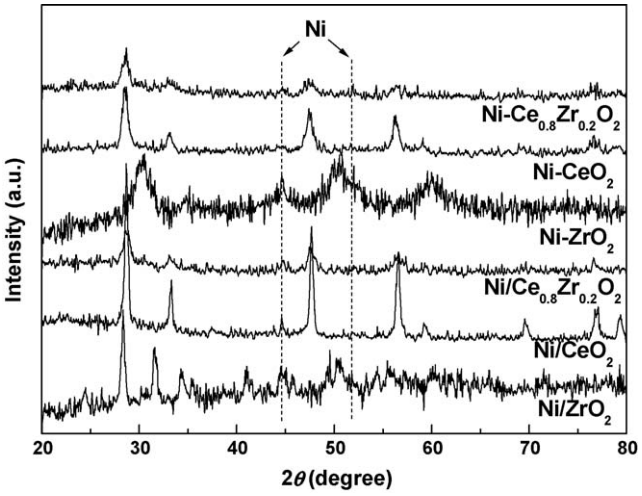

Fig. 2. XRD patterns of reduced co-precipitated and impregnated catalysts.

Compared with the impregnated catalysts, the co-precipitated catalysts show different patterns. For the Ni–ZrO_2 catalyst, one peak appears at 420 °C and the other peak is very broad. The first is from the reduction of free NiO species, the second peak from the reduction of complex NiO species, which have relatively strong interaction with the support. This indicates that the co-precipitated Ni–ZrO_2 catalyst has SMSI, compared with the impregnated Ni/ZrO_2 catalyst. In the case of Ni–CeO_2 catalyst, the first peak appears at 370 °C. It is known that NiO can be reduced easily in the presence of CeO_2 [29]. The second broad peak can be attributed to the reduction of complex NiO species. For the Ni–$Ce_{0.8}Zr_{0.2}O_2$ catalyst, it also shows complex peaks with peak maxima at 450, 630, 810, and 960 °C. The first peak originates from the reduction of relatively free NiO species. The second peak is from the reduction of complex NiO species. The third peak is assigned to the reduction of segregated CeO_2 and the last peak is due to the presence of carbonate-type species [19]. According to the above results, it has been confirmed that the co-precipitated catalysts have stronger metal to support interaction than the impregnated ones.

3.2. Reaction results

The reaction results for CH_4 conversion with time on stream are illustrated in Fig. 4. Both co-precipitated Ni–$Ce_{0.8}Zr_{0.2}O_2$ and Ni–CeO_2 catalysts exhibited the highest CH_4 conversion with stability. On the contrary, impregnated Ni/$Ce_{0.8}Zr_{0.2}O_2$ and Ni/CeO_2 catalysts slowly deactivated with time on stream. It is most likely that Ni dispersion is very important for the catalyst to have high activity. According to the dispersion data in Table 1, co-precipitated Ni–

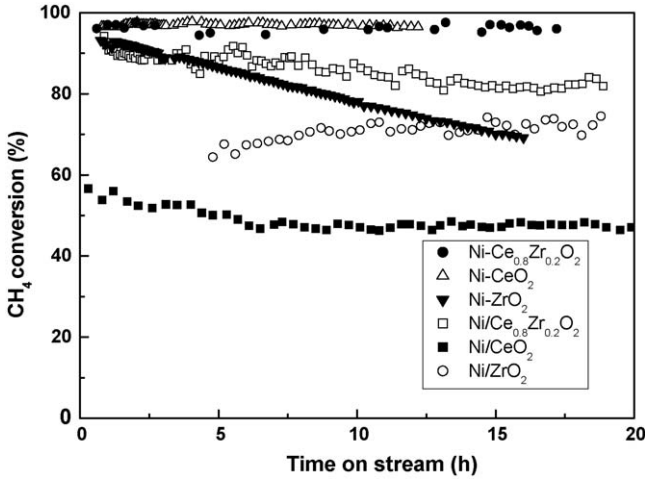

Fig. 4. CH_4 conversion with time on stream over co-precipitated and impregnated catalysts (T = 800 °C, GHSV = 265,000 $cm^3/h\ g_{cat}$).

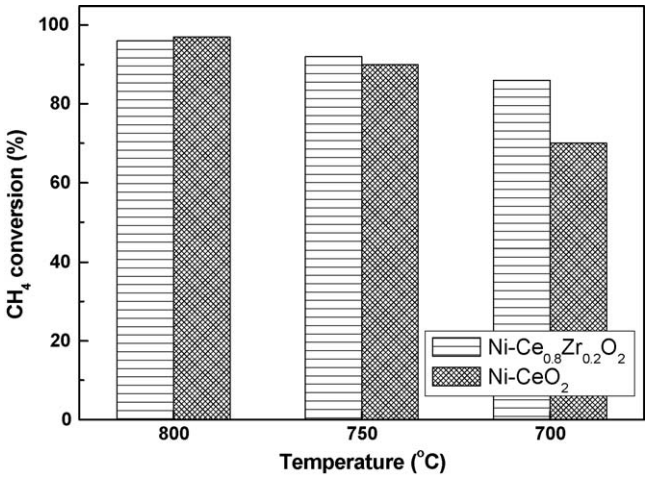

Fig. 5. CH_4 conversion with reaction temperature over co-precipitated Ni–$Ce_{0.8}Zr_{0.2}O_2$ and Ni–CeO_2 catalysts (GHSV = 265,000 $cm^3/h\ g_{cat}$).

$Ce_{0.8}Zr_{0.2}O_2$ and Ni–CeO_2 catalysts have higher Ni dispersion than the other catalysts. Another significant factor is SMSI. According to the TPR curves, the co-precipitated catalysts have stronger metal to support interaction than the impregnated ones. In another word, the impregnated catalysts have larger portion of relatively free NiO species, compared with the co-precipitated catalysts. It is possible that free NiO species agglomerate during reduction and reaction owing to sintering at high temperatures. In reality, reduced co-precipitated Ni–$Ce_{0.8}Zr_{0.2}O_2$ and Ni–CeO_2 catalysts do not show distinct Ni peaks, as shown in Fig. 2. On the contrary, the other catalysts show Ni peaks in XRD patterns. As a result, both co-precipitated Ni–$Ce_{0.8}Zr_{0.2}O_2$ and Ni–CeO_2 catalysts showed relatively stable activity with time on stream.

In the case of co-precipitated Ni–ZrO_2, it deactivated with time on stream. For impregnated Ni/ZrO_2 catalyst, it did not show high activity. Thus, it has been confirmed that the conventional impregnation method is not effective to prepare catalysts having good activity and stability in CSCRM. It is also concluded that CeO_2 plays an important role in having high activity as well as stability in CSCRM. This is due to high oxygen storage capacity of CeO_2, which stores and releases reversibly active oxygen species depending on the reaction condition. CeO_2 can be partially reduced under reductive environment, giving active oxygen species, which react with surface carbon, resulting in preventing coke formation in CSCRM [39]. The partially reduced ceria can be re-oxidized by receiving active oxygen species from water and/or CO_2 molecules.

Both co-precipitated Ni–$Ce_{0.8}Zr_{0.2}O_2$ and Ni–CeO_2 catalysts exhibited almost equilibrium CH_4 conversion (97%) at 800 °C and 265,000 $cm^3/h\ g_{cat}$ GHSV. Both catalysts showed stable activity for more than 20 h without significant catalyst deactivation. To our knowledge, it is very rare that supported Ni catalysts show such a high activity and stability under the condition of GHSV = 265,000 $cm^3/h\ g_{cat}$ in CSCRM. According to the above reaction results, it is obvious that $Ce_{0.8}Zr_{0.2}O_2$ and CeO_2 are the promising supports in CSCRM.

To compare co-precipitated Ni–$Ce_{0.8}Zr_{0.2}O_2$ and Ni–CeO_2 catalysts precisely, the reaction temperature was changed from 800 to 700 °C at the same GHSV. Fig. 5 shows CH_4 conversion with reaction temperature over co-precipitated Ni–$Ce_{0.8}$–$Zr_{0.2}O_2$ and Ni–CeO_2 catalysts. The detailed reaction results of the co-precipitated Ni–$Ce_{0.8}$–$Zr_{0.2}O_2$ and Ni–CeO_2 catalysts are summarized in Table 2. Both catalysts exhibited almost equilibrium CH_4 and CO_2 conversion at 800 °C. The Ni–$Ce_{0.8}$–$Zr_{0.2}O_2$ catalyst still showed equilibrium CH_4 and CO_2 conversion at 750 °C, while the Ni–CeO_2 catalyst showed slightly low CH_4 and CO_2 conversion. At 700 °C, the activity of the Ni–$Ce_{0.8}$–$Zr_{0.2}O_2$ catalyst is higher than that of the Ni–CeO_2 catalyst. Thus, it has been confirmed that the co-precipitated Ni–$Ce_{0.8}$–$Zr_{0.2}O_2$ catalyst is the best candidate catalyst in CSCRM among the catalysts tested in this study. According to the above results, it is concluded that Ni–$Ce_{0.8}Zr_{0.2}O_2$ solid solution prepared by the co-precipitation method is highly effective in CSCRM.

For the F–T synthesis in GTL, the H_2/CO ratio in the product should be 2. Table 3 summarizes H_2/CO ratio with reaction temperature over co-precipitated Ni–$Ce_{0.8}$–$Zr_{0.2}O_2$ and Ni–CeO_2 catalysts. It is obvious that the H_2/CO ratio in the product synthesis gas has been controlled to be around 2 from 800 to 700 °C. Thus, it has been confirmed that the desirable H_2/CO ratio for the F–T synthesis was achieved in this reaction conditions (feed $H_2O/CO_2/CH_4$ = 0.8/0.4/1.0).

It is likely that the outstanding activity and stability of the co-precipitated Ni–$Ce_{0.8}Zr_{0.2}O_2$ catalyst is related to high surface area, nano-crystalline size of both $Ce_{0.8}Zr_{0.2}O_2$ support and NiO, better dispersion of nano-sized NiO crystallites in $Ce_{0.8}Zr_{0.2}O_2$ support resulting in strong metal to support interaction, and enhanced oxygen transfer during CSCRM. The intimate contact between Ni and $Ce_{0.8}Zr_{0.2}O_2$ would enhance oxygen transfer from cubic $Ce_{0.8}Zr_{0.2}O_2$ support to Ni, which is beneficial to prevent carbon formation during CSCRM. It is known that the cubic $Ce_{0.8}Zr_{0.2}O_2$

Table 2
CH_4 and CO_2 conversion with reaction temperature over co-precipitated Ni–$Ce_{0.8}$–$Zr_{0.2}O_2$ and Ni–CeO_2 catalysts.

Catalyst	800 °C		750 °C		700 °C	
	X_{CH_4}	X_{CO_2}	X_{CH_4}	X_{CO_2}	X_{CH_4}	X_{CO_2}
Ni–$Ce_{0.8}Zr_{0.2}O_2$	96	80	92	73	86	54
Ni–CeO_2	97	79	90	71	70	42
Equilibrium	97	79	92	72	86	52

Unit: % (error <0.5).

Table 3
H_2/CO ratio with reaction temperature over co-precipitated Ni–$Ce_{0.8}$–$Zr_{0.2}O_2$ and Ni–CeO_2 catalysts.

Catalyst	800 °C	750 °C	700 °C
Ni–$Ce_{0.8}Zr_{0.2}O_2$	1.9	1.9	2.0
Ni–CeO_2	1.9	1.9	2.1
Equilibrium	2.0	2.0	2.4

Error <0.05.

solid solution has the redox ability [39]. The redox ability of $Ce_{0.8}Zr_{0.2}O_2$ solid solution is higher than that of CeO_2 alone [39]. A higher rate of oxygen transfer effectively prevents carbon formation in severe conditions.

4. Conclusions

The co-precipitation method is a promising method to prepare highly active and stable catalysts with high surface area, better dispersion of metal, and intimate contact between metal and support for CSCRM compared with the conventional impregnation method. Co-precipitated Ni–$Ce_{0.8}Zr_{0.2}O_2$ exhibited the highest activity as well as stability due to nano-sized crystallite of both $Ce_{0.8}Zr_{0.2}O_2$ and NiO resulting in intimate contact between Ni and support, better Ni dispersion, and enhanced oxygen transfer during the reaction.

Acknowledgments

The authors would like to acknowledge the financial support of KEMCO and GTL Technology Development Consortium (Korea National Oil Corp., Daelim Industrial Co., Ltd., Doosan Mecatec Co., Ltd., Hyundai Engineering Co. Ltd. and SK Energy Co. Ltd.) under "Energy & Resources Technology Development Programs" of the Ministry of Knowledge Economy, Republic of Korea.

References

[1] K. Aasberg-Petersen, T.S. Christensen, I. Dybkjaer, J. Sehested, M. Ostberg, R.M. Coertzen, M.J. Keyser, A.P. Steynberg, Stud. Surf. Sci. Catal. 152 (2004) 258.
[2] J.R. Rostrup-Nielsen, in: J.R. Anderson, M. Boudart (Eds.), Catalysis Science and Technology, vol. 5, Springer, Berlin, 1984, p. 1.
[3] M.A. Peña, J.P. Gómez, J.L.G. Fierro, Appl. Catal. A 144 (1996) 7.
[4] H.-S. Roh, K.-W. Jun, W.-S. Dong, J.-S. Chang, S.-E. Park, Y.-I. Joe, J. Mol. Catal. A 181 (2002) 137.
[5] H.-S. Roh, K.-W. Jun, S.-E. Park, Appl. Catal. A 251 (2003) 275.
[6] Z.-W. Liu, K.-W. Jun, H.-S. Roh, S.-E. Park, J. Power Sources 111 (2002) 283.
[7] S.C. Tsang, J.B. Claridge, M.L.H. Green, Catal. Today 23 (1995) 3.
[8] A.T. Ashcroft, A.K. Cheetham, J.S. Foord, M.L.H. Green, C.P. Grey, A.J. Murrell, P.D.F. Vernon, Nature 344 (1990) 319.
[9] V.R. Choudhary, A.S. Mamman, D. Sansare, Angew. Chem. Int. Ed. Engl. 31 (1992) 1189.
[10] H.-S. Roh, W.-S. Dong, K.-W. Jun, S.-E. Park, Chem. Lett. (2001) 88.
[11] H.-S. Roh, K.-W. Jun, W.-S. Dong, S.-E. Park, Y.-I. Joe, Chem. Lett. (2001) 666.
[12] Q.-H. Zhang, Y. Li, B.-Q. Xu, Catal. Today 98 (2004) 601.
[13] H.-S. Roh, K.Y. Koo, J.H. Jeong, Y.T. Seo, D.J. Seo, Y.-S. Seo, W.L. Yoon, S.B. Park, Catal. Lett. 117 (2007) 85.
[14] K.Y. Koo, H.-S. Roh, Y.T. Seo, D.J. Seo, W.L. Yoon, S.B. Park, Appl. Catal. A 340 (2008) 183.
[15] K.Y. Koo, H.-S. Roh, Y.T. Seo, D.J. Seo, W.L. Yoon, S.B. Park, Int. J. Hydrogen Energy 33 (2008) 2036.
[16] H.-S. Roh, K.Y. Koo, U.D. Joshi, W.L. Yoon, Catal. Lett. 125 (2008) 283.
[17] B.-Q. Xu, J.-M. Wei, H.-Y. Wang, K.-Q. Sun, Q.-M. Zhu, Catal. Today 68 (2001) 217.
[18] H.-S. Roh, H.S. Potdar, K.-W. Jun, Catal. Today 93–95 (2004) 39.
[19] H.-S. Roh, H.S. Potdar, K.-W. Jun, J.-W. Kim, Y.-S. Oh, Appl. Catal. A 276 (2004) 231.
[20] A. Trovarelli, C. de Leitenburg, G. Dolcetti, Chemtech (June) (1997) 32.
[21] J. Kaspar, P. Fornasiero, M. Graziani, Catal. Today 50 (1999) 285.
[22] S. Rossignol, F. Gerard, D. Duprez, J. Mater. Chem. 9 (1999) 1615.
[23] C. de Leitenburg, A. Trovarelli, J.L. Lorea, F. Cavani, G. Bini, Appl. Catal. A 139 (1996) 161.
[24] E. Bekyarova, P. Fornasiero, J. Kaspar, M. Graziani, Catal. Today 45 (1998) 178.
[25] D. Terribile, A. Trovarelli, C. de Leitenburg, A. Primareva, G. Dolcetti, Catal. Today 47 (1999) 133.
[26] J.A. Lercher, J.H. Bitter, W. Hally, W. Niessen, K. Seshan, Stud. Surf. Sci. Catal. 101 (1996) 463.
[27] X. Li, J.-S. Chang, S.-E. Park, Chem. Lett. (1999) 1099.
[28] X. Li, J.-S. Chang, M. Tian, S.-E. Park, Appl. Organometal. Chem. 15 (2001) 109.
[29] H.-S. Roh, K.-W. Jun, W.-S. Dong, S.-E. Park, Y.S. Baek, Catal. Lett. 74 (2001) 31.
[30] W.-S. Dong, H.-S. Roh, K.-W. Jun, S.-E. Park, Y.-S. Oh, Appl. Catal. A 226 (2002) 63.
[31] J.A. Montoya, E. Romero-Pascual, C. Gimon, P.D. Angel, A. Monzon, Catal. Today 63 (2000) 71.
[32] H.-S. Roh, Y. Wang, D.L. King, A. Platon, Y.-H. Chin, Catal. Lett. 108 (2006) 15.
[33] H.-S. Roh, A. Platon, Y. Wang, D.L. King, Catal. Lett. 110 (2006) 1.
[34] A. Platon, H.-S. Roh, D.L. King, Y. Wang, Top. Catal. 46 (2007) 374.
[35] H.-S. Roh, Y. Wang, D.L. King, Top. Catal. 49 (2008) 32.
[36] J. Kugai, S. Velu, C. Song, Catal. Lett. 101 (2005) 255.
[37] J. Kugai, V. Subramani, C. Song, M.H. Engelhard, Y.-H. Chin, J. Catal. 238 (2006) 309.
[38] H.S. Potdar, H.-S. Roh, K.-W. Jun, M. Ji, Z.-W. Liu, Catal. Lett. 84 (2002) 95.
[39] K.-W. Jun, H.-S. Roh, K.V.R. Chary, Catal. Surv. Asia 11 (2007) 97.